FLOODING LIMITS IN A SIMULATED NUCLEAR REACTOR HOT LEG

by

SUSAN M. KROLEWSKI

SUBMITTED IN PARTIAL FULFILMENT
OF THE REQUIREMENTS FOR THE
DEGREE OF

BACHELOR OF SCIENCE

at the

MASSACHUSETTS INSTITUTE OF TECHNOLOGY

AUGUST 1980

Signature of Author _____
Department of Mechanical Engineering
August 9, 1980

Certified by _____
Peter Griffith
Thesis Advisor

Accepted by _____
Chairman, Department Committee

FLOODING LIMITS IN SIMULATED NUCLEAR REACTOR HOT LEG

by

SUSAN M. KROLEWSKI

Submitted to the Department of Mechanical Engineering on August 9, 1980 in partial fulfillment of the requirements for the Degree of Bachelor of Science in Mechanical Engineering

ABSTRACT

During a small break LOCA one mode of decay heat removal is reflux cooling. When this occurs steam is evolved in the core, passes to the steam generators, is condensed and the condensate returns through the hot leg to the core. Experiments were performed to determine the flooding limits for two phase air/water flow in a simulated nuclear reactor hot leg. Since there is no standard hot leg geometry, five different configurations were tested. It was found that the geometry of hot leg had a significant effect on the flooding limits. Flooding data plotted on basis of square roots of the non-dimensional superficial velocities for one configuration was compared with the results observed by Wallis (1969) for vertical tubes with reasonable agreement. The range of hysteresis, however, was unusually high and possibly a function of change in flow from open channel supercritical to subcritical.

Thesis Advisor: Professor Peter Griffith

TABLE OF CONTENTS

LIST OF FIGURES AND TABLES

NOMENCLATURE

A_{TOTAL}	Total Cross sectional Area of Pipe (FT^2)
A_{WATER}	Water Filled Cross Sectional Area of Pipe (FT^2)
C	Y-intercept of Non-dimensional Superficial Velocity Flooding Curve
D	Diameter of Pipe (FT)
Fr	Froude Number
g	Gravitational Acceleration (32.2 FT/SEC^2)
h	Height of Water in Square Channel (FT)
h_{MAX}	Height of Water in Pipe (FT)
J_F	Superficial Velocity of Water (FT/SEC)
J_G	Superficial Velocity of Air (FT/SEC)
J_F^*	Non-dimensional Superficial Velocity of Water
J_G^*	Non-dimensional Superficial Velocity of Air
m	Slope of Non-dimensional Superficial Velocity Flooding Curve
N_L	Grashoff Number
Q	Volumetric Flow Rate (FT^3/SEC)
R	Radius of Pipe (FT)
u_1	Liquid Viscosity
V	Velocity of Water (FT/SEC^2)
ρ_F	Density of Water (LB/FT^3)
ρ_G	Density of Air (LB/FT^3)

INTRODUCTION

It is essential for all nuclear reactors to continuously provide sufficient cooling to the core in order to prevent destruction of the clad and the release of radioactive materials to the environment. The emergency core cooling system (ECCS) in a PWR is designed to provide adequate core cooling after an accident. If the coolant level in the core decreases, ECCS water is injected into the core from storage tanks through the cold legs. The ECCS, however, can not provide infinite water supplies to the core. Due to its infrequent use, it is also prone to mechanical malfunctions. It is therefore worthwhile to investigate additional means of core cooling that would not require additional equipment.

A loss of coolant accident (LOCA) is caused by a break in one of the primary recirculation loops. A rapid depressurization from approximately 2200 psi to containment pressure causes flashing of primary coolant to steam. As a result of this, the primary coolant exists as a two phase mixture of steam and water. One mode of cooling that has been postulated is that steam will be evolved and travel out of the core through the hot leg and into the steam generator and then condense. The condensate would then flow down the steam generator, collect at the bottom and eventually flow back to the core through the hot leg. The condensate could then augment the ECCS reflood process.

There are two limitations on the mass flow of condensate

flowing back to the core. The first involves the heat transfor capabilities of the steam generator. The second is the limit of countercurrent steam/condensate flow possible in the hot leg region of the primary coolant system. This limit is defined as flooding. Beyond the flooding point, increasing the flow of either phase will cause either a change in flow regime or a rejection of excess material at the ends of the flow passage. The flooding point is the result of a sudden and dramatic instability which increases the pressure gradient by an order of magnitude.

Wallis(1969) used an empirical approach to correlate flooding data for flow in vertical tubes. Wallis based his correlations on the non-dimensional superficial velocities, J_G^* and J_F^*, defined by

$$J_G^* = \left[\frac{J_G \rho_F}{gD(\rho_F - \rho_G)} \right]^{\frac{1}{2}}$$

and

$$J_F^* = \left[\frac{J_F \rho_F}{gD(\rho_F - \rho_G)} \right]^{\frac{1}{2}}$$

J_G^* and J_F^* are analogous to the Froude number, Fr, which represents the ratio of inertial forces to gravity forces and is given by

$$Fr = \frac{V}{\sqrt{gh}}$$

According to Wallis, the flooding points for vertical pipes are given by

$$J_G^{*\frac{1}{2}} + mJ_F^{*\frac{1}{2}} = C$$

where m is the slope and C is the y-intercept of the non-dimensional flooding curve. The slope and the y-intercept are related to the Grashoff number, N_L, which represents the ratio of gravity forces to viscous forces and is given by

$$N_L = \frac{\rho_F g D^3 (\rho_F - \rho_G)^{\frac{1}{2}}}{u_L^2}$$

For high N_L, the gravity forces are more significant, m is almost unity and $.75 < C < 1$. For small N_L, the gravity forces are less significant, $m = 5.6 N_L^{-\frac{1}{2}}$ and C is a function of the inlet and outlet conditions.

Some hystersis was observed in many flooding experiments. The air flow rate, J_G, had to be reduced before the tube would return to smooth operating conditions. The range of hystersis was between the lines

$$J_F^{*\frac{1}{2}} + J_G^{*\frac{1}{2}} = 1$$

and

$$J_F^{*\frac{1}{2}} + J_G^{*\frac{1}{2}} = .88$$

The geometry of hot legs, however, is more complicated and varies from nuclear reactor to reactor. It is not certain whether Wallis's correlations can be used to determine flooding limits in hot legs. This thesis will experimentally determine the flooding limits of two phase air/water flow in five geometrically different simulated nuclear reactor hot legs and compare the results to Wallis's correlations.

APPARATUS

The test apparatus models the countercurrent two phase flow of steam and condensate in the hot leg region of the reactor primary coolant system. Figure 1. is a schematic diagram of a primary system of a typical C-E two loop PWR and indicates the section modelled by the test apparatus. Since only the fluid mechanics aspect was of interest, the steam/condensate flow was simulated by air/water flow.

The test section of the apparatus was constructed from two inch diameter plexiglass tubing and PVC fittings. Plexiglass was selected primarily to allow for flow pattern observation. Since not all reactors have the same primary loop geometry, five different pipe configurations as shown in Figures 2, 3, 4, 5 and 6 were used. In each case a 24" horizontal section of pipe simulated the hot leg piping. One end was connected to a elbow and pipe configuration simulating the different entrances into the steam generator. The pipe was directed upward through a metal container simulating the bottom of the steam generator. On the other end of the horizontal pipe, two different fitting and pipe combinations were used to simulate the junction of the hot leg with the core. This end was directed downward and submerged in a weigh tank simulating the core.

To simulate the flow of condensate down the steam generator, water was poured into the metal container and allowed to pour over the sides of the piping. The mass flow rate was

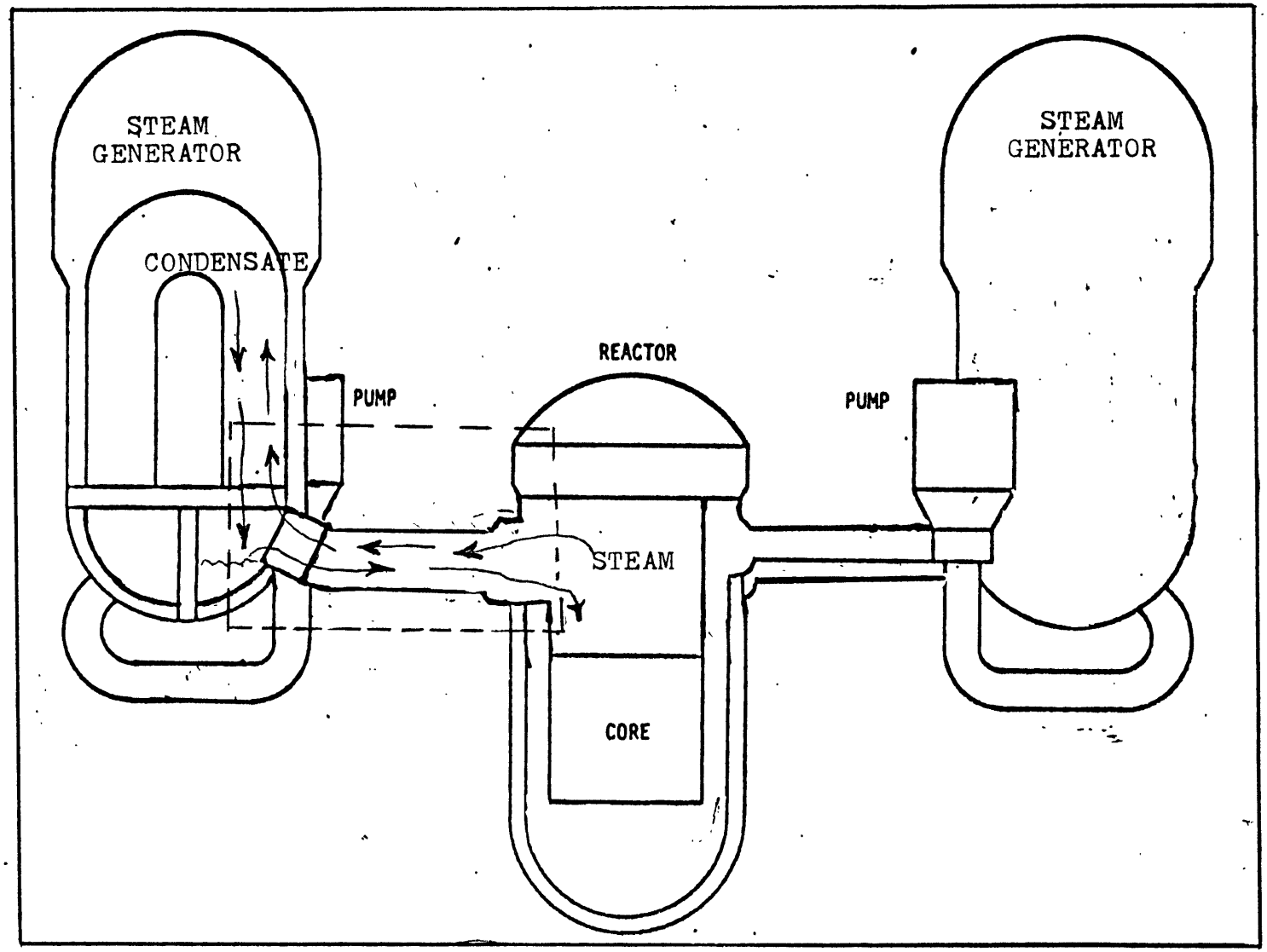

FIGURE 1. SCHEMATIC DIAGRAM OF THE PRIMARY SYSTEM OF A TWO LOOP PWR

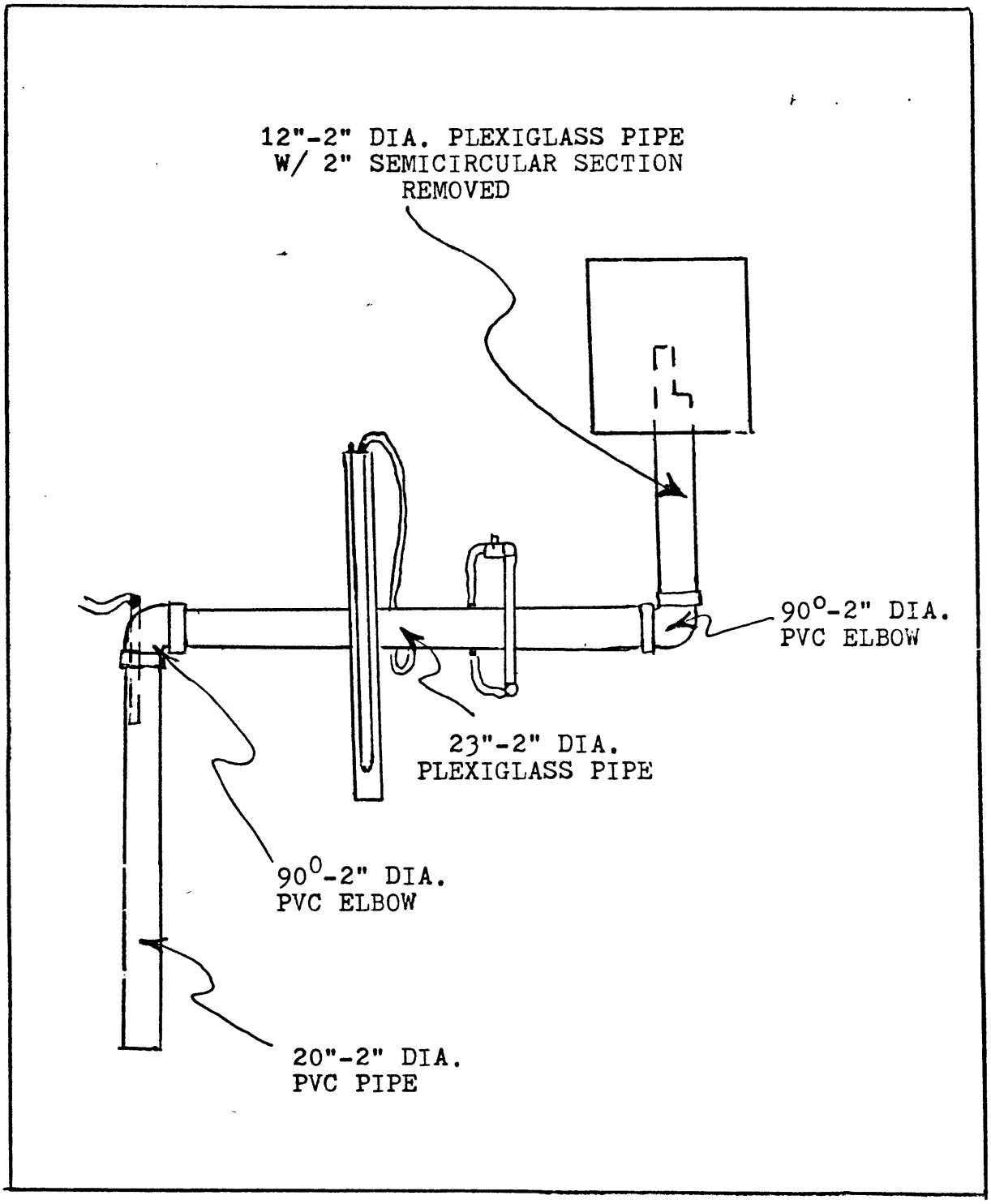

FIGURE 2. CONFIGURATION A OF TEST SECTION

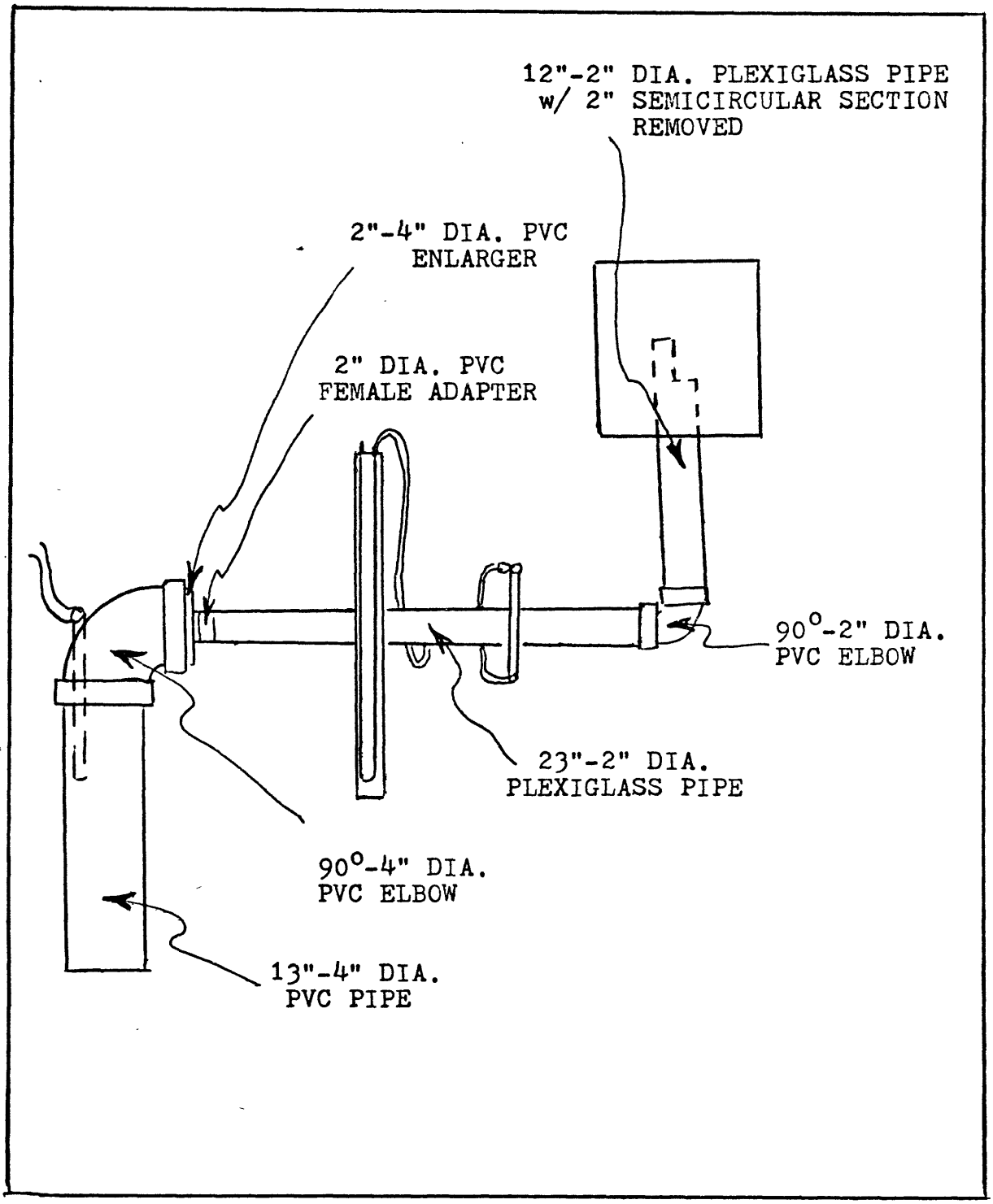

FIGURE 3. CONFIGURATION B OF TEST SECTION

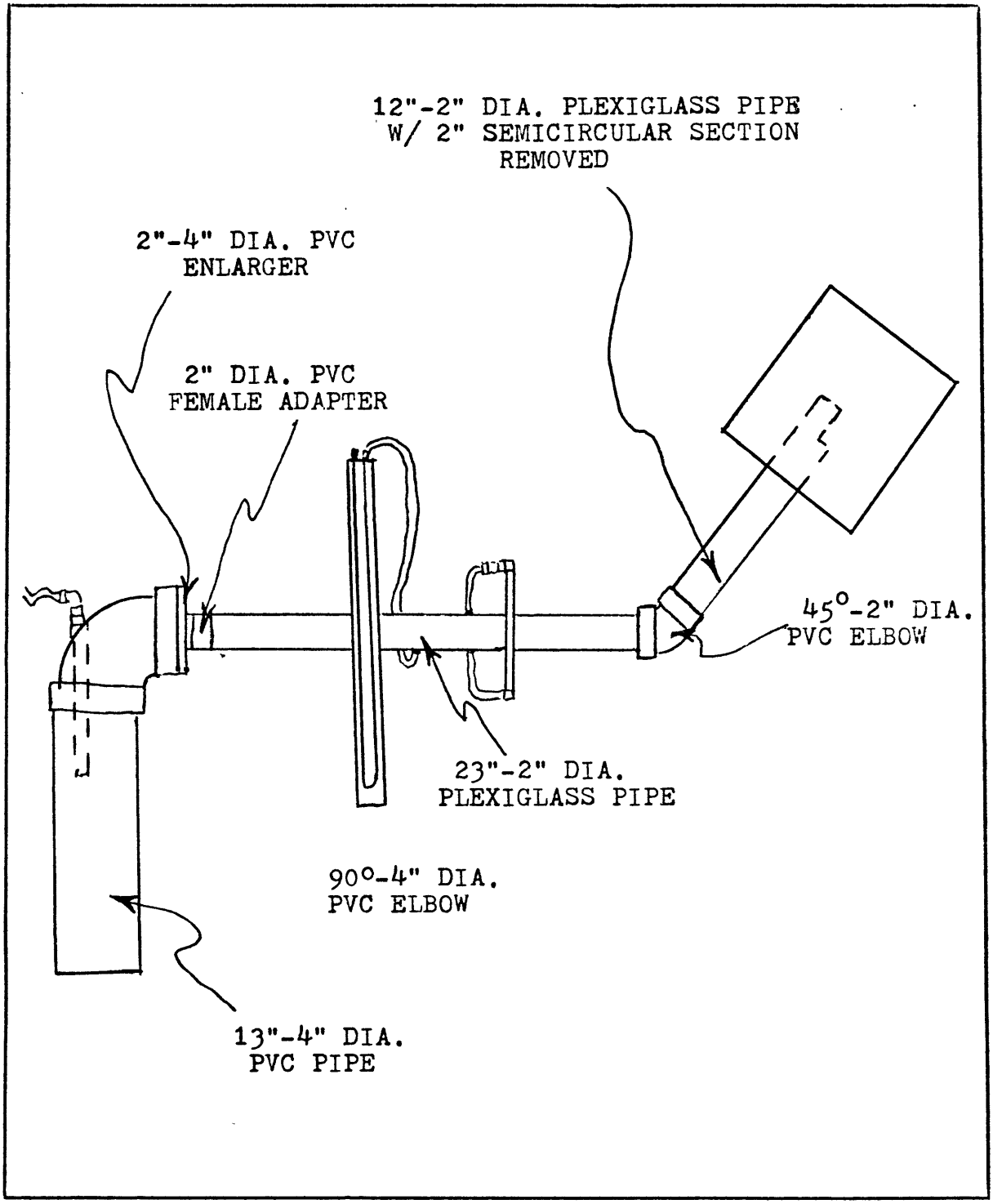

FIGURE 4. CONFIGURATION C OF TEST SECTION

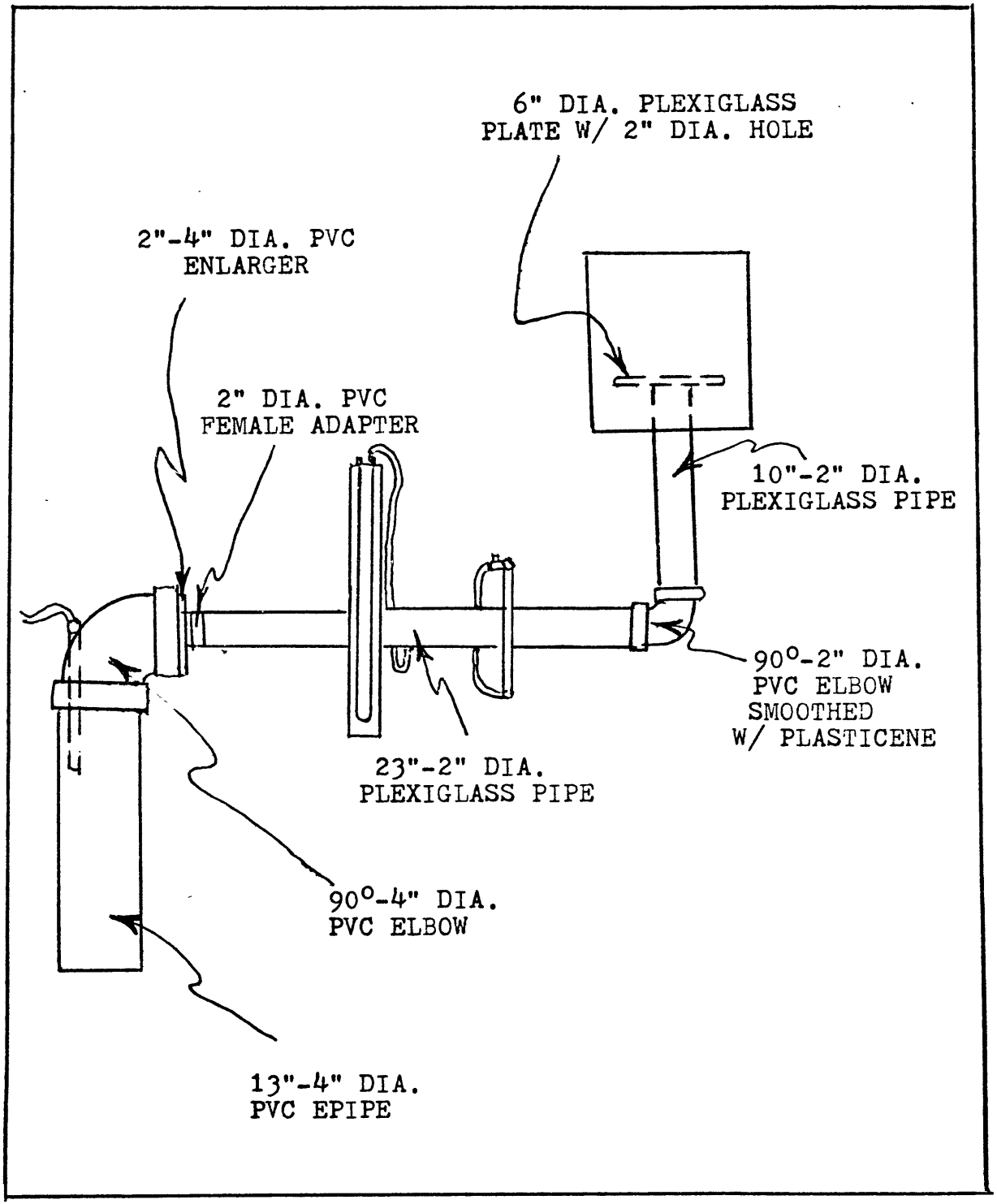

FIGURE 5 . CONFIGURATION D OF TEST SECTION

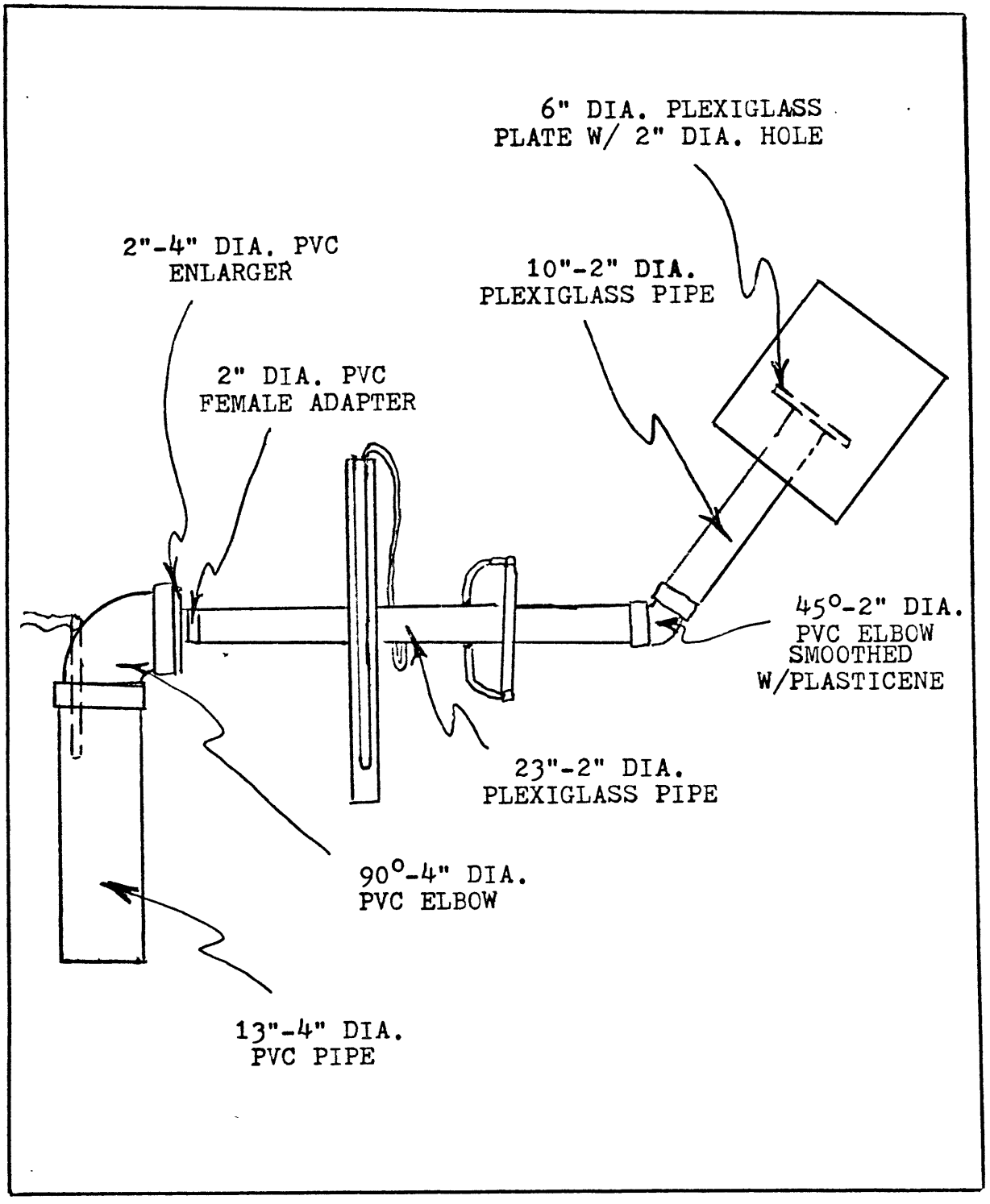

FIGURE 6. CONFIGURATION E OF TEST SECTION

determined by weighing the accumulation in the weigh tank over a measured time period. To simulate the flow of steam, air was injected into the system through an inlet tube located in the vertical pipe submerged in the weigh tank. Air flow rate was measured by two Fisher and Porter flowmeters, FP-½-27-G-10/55 and FP-1-35-6-10/83 hooked up in parallel. They were used for low and high ranges of air flow respectively. Since the flowmeters were calibrated at atmosphere, it was necessary to determine the operating pressure of the system. A mercury manometer was attached to the inlet of the two flowmeters to determine the operating pressure. The operating flow rate was equal to the flow rate at atmospheric pressure times the square root of the operating pressure divided by the atmospheric pressure.

A water manometer was attached to the bottom of the horizontal plexiglass section to determine the pressure of system as water and air velocities were varied. Two small diameter taps were drilled into the top and bottom of the horizontal plexiglass tubing. A piece of polyflow tubing was connected between each hole and the end of a ½ inch diameter vertical glass tube which was mounted along side the test section. The tube was used to determine the level of water in the horizontal pipe. A valve was placed at the top of the glass tube to permit damping of rapid height oscillations.

Figure 7 shows the entire experimental setup.

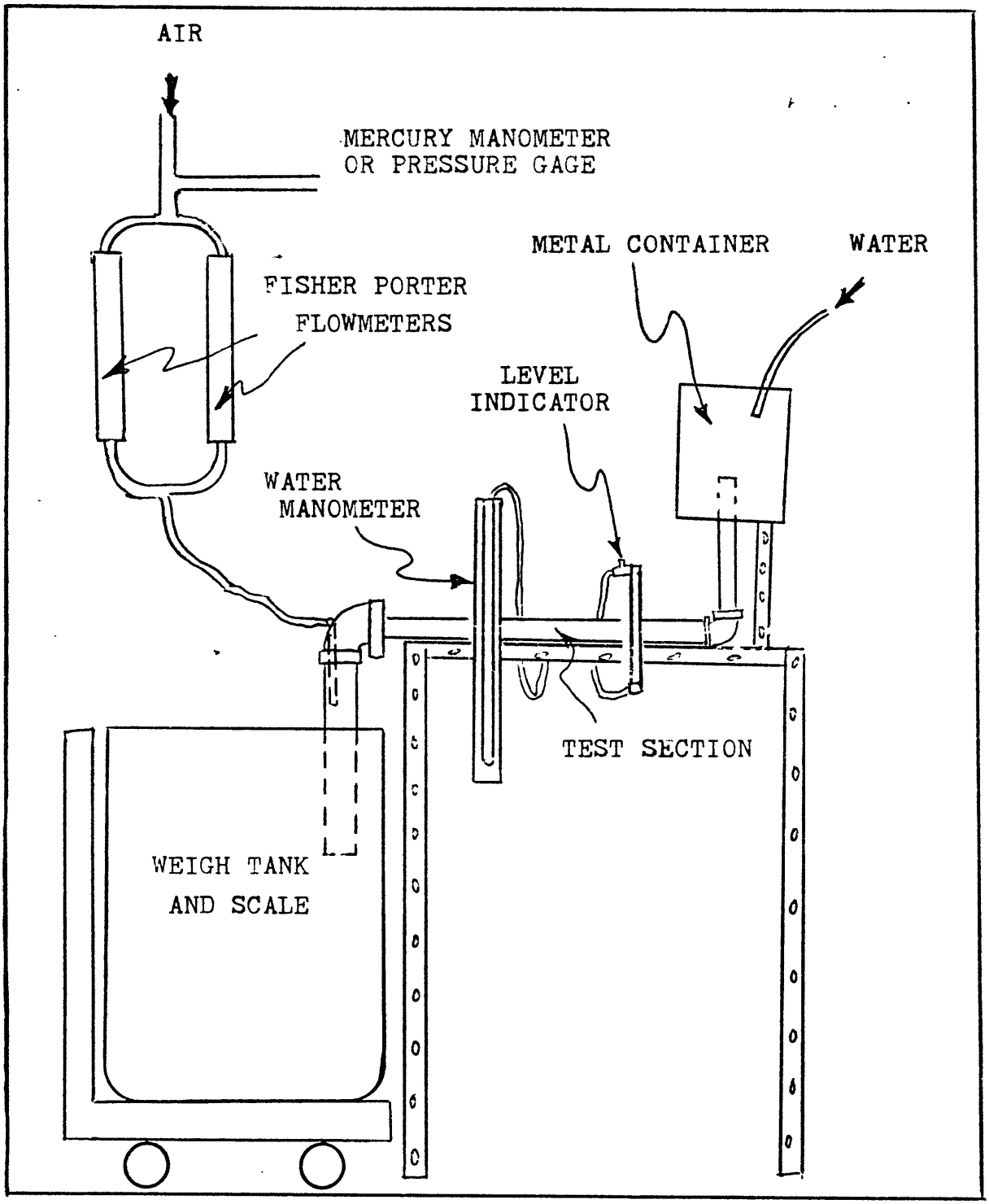

FIGURE 7. EXPERIMENTAL SETUP

EXPERIMENTAL PROCEDURE

Tests were performed to determine the air flow rates which initiated and terminated flooding for several different water flow rates for each of the five "hot leg" configurations.

Before each test run, the water flow rate was determined by weighing a sample collected in the weigh tank over a measured period of time. The water flow rate was then held constant and the air flow was slowly increased until a sudden increase in pressure was detected on the water manometer. This change in pressure indicated that the flooding limit had been reached. The flooding location was recorded. To determine the range of hystersis, the air flow rate was slowly decreased until the pipe returned to smooth operating conditions.

An additional test was performed on Configurations E to enable calculations of the liquid Froude numbers at both of the flooding limits. For five different constant water flow rates, the height of water in the vertical tube of level indicator for limit as J_G is increased and the limit as J_G was decreased.

RESULTS AND DISCUSSION

The air flow rate, J_G, was varied for several different water flow rates, J_F, in each of the five configurations to determine the flooding limits. The flooding curves for various pipe configurations are shown in Figures 8, 9, 10, 11 and 12. Very definite transition points from one flooding pattern to another were observed for Configurations A, B and C. Configurations D and E flooded only at one location. The range of hystersis was significant only in configurations C and E which had 45^0 elbows at one end of the test section. The hystersis effect was much more significant than those reported by Wallis's.

The composite plot in Figure 13 directly compares the flooding limit as J_G is increased for all five configurations. According to Wallis, the flooding curve slope and y-intercepts are directly related to the liquid viscosity, the density of liquid and gas and the geometry of the pipe. Since the fluid properties are identical for all five configurations, the differences in the flooding curve are due to the change in geometry. The transitions from one flooding pattern to another is also indicated in Figure 13. Changes in flooding location cause a slight change in the slope of flooding curve. The flooding limit for each pipe fitting is probably slightly different. The configurations floods at the lowest limit. When flooding occurs at two locations at once the water flow rate limit is slightly higher since water is partially held

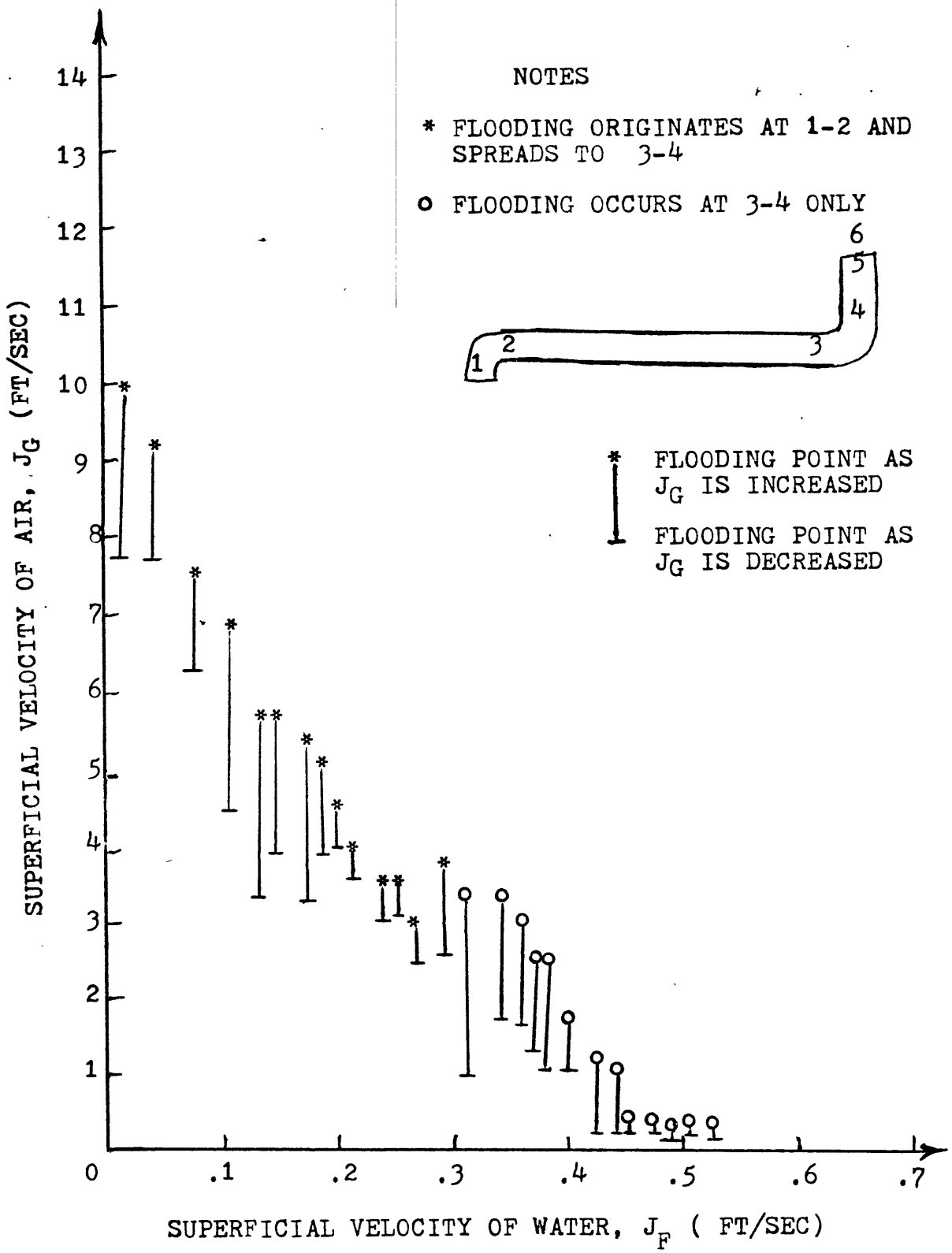

FIGURE 8. FLOODING CURVE FOR CONFIGURATION A

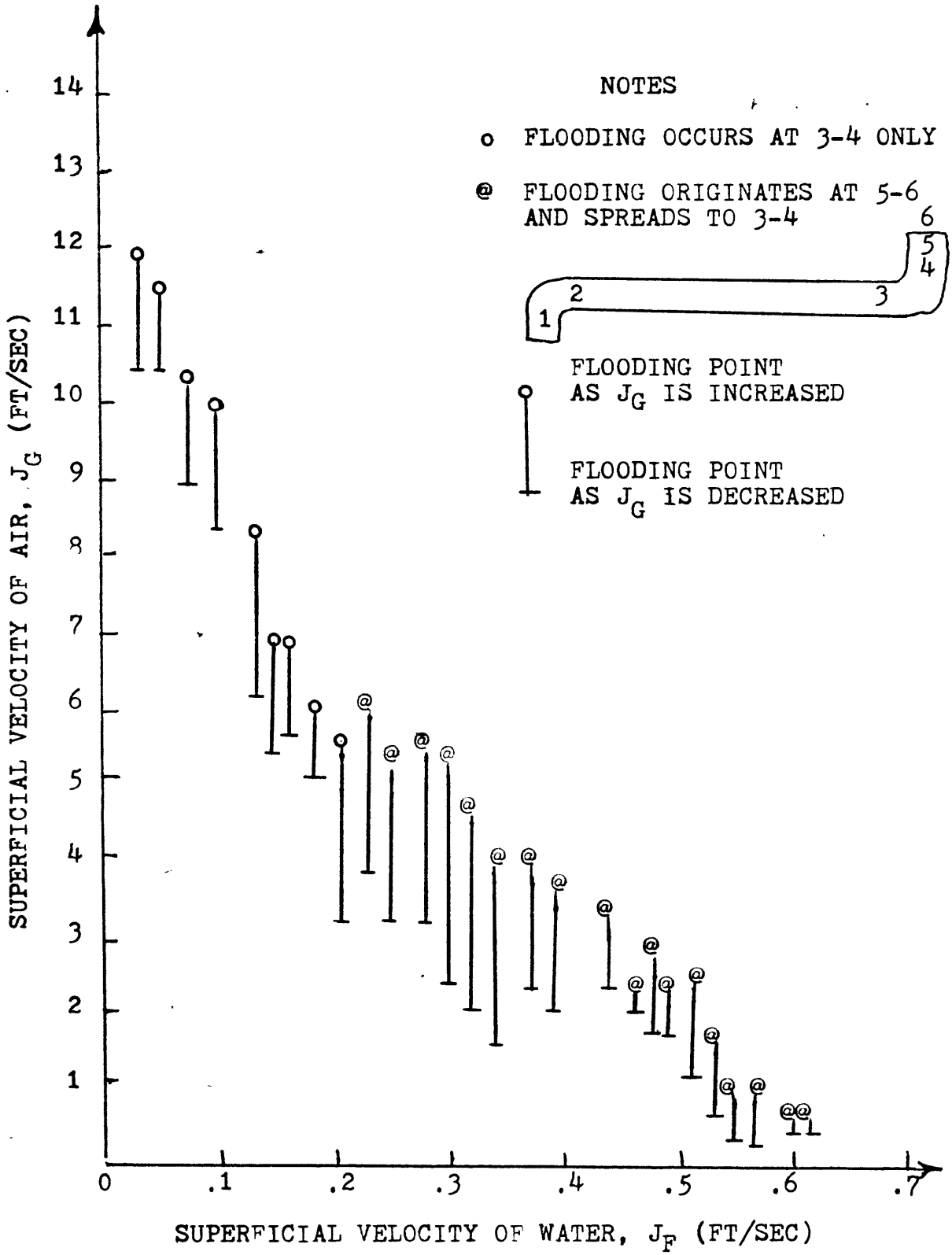

FIGURE 9. FLOODING CURVE FOR CONFIGURATION B

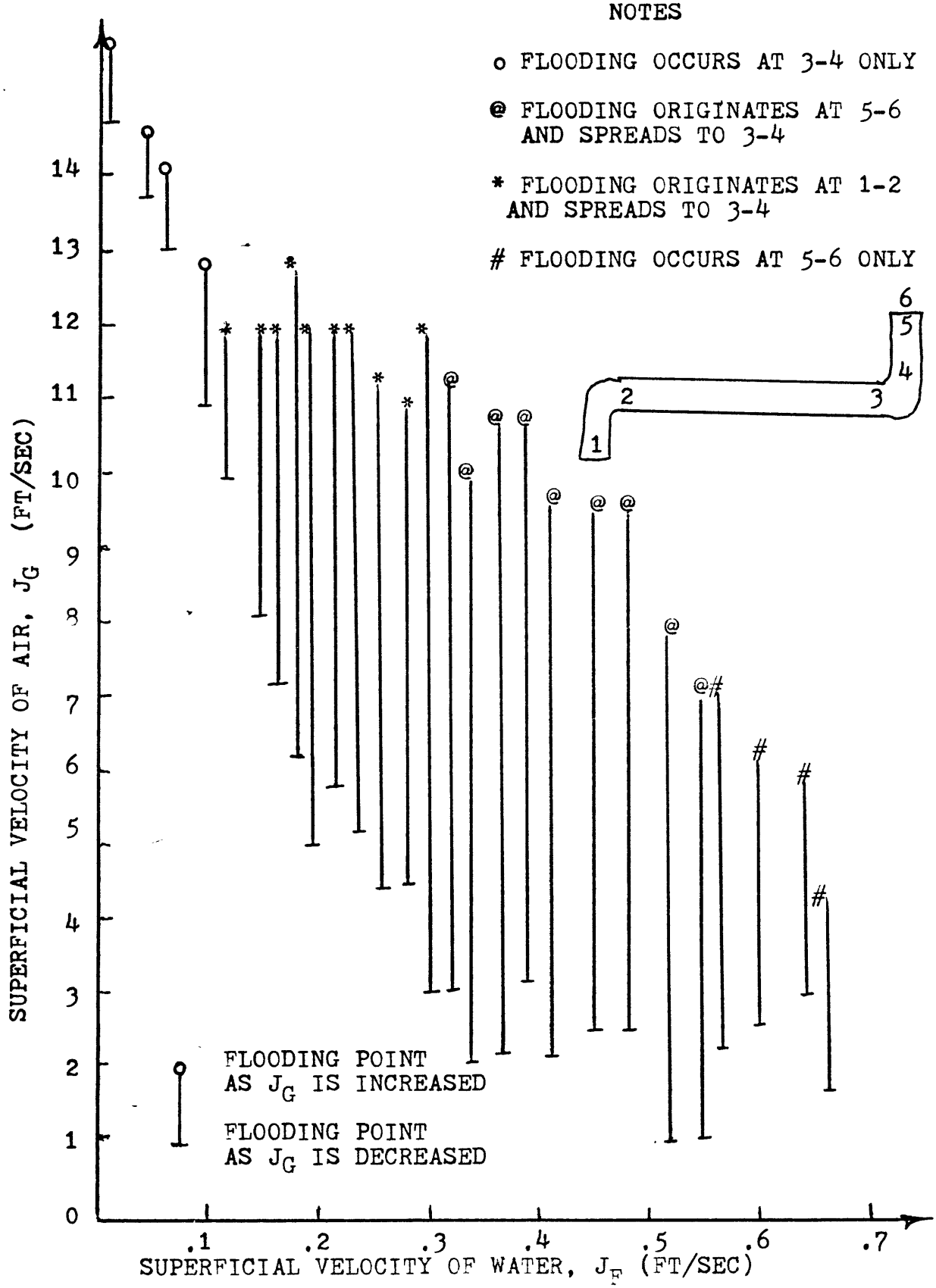

FIGURE 10. FLOODING CURVE FOR CONFIGURATION C

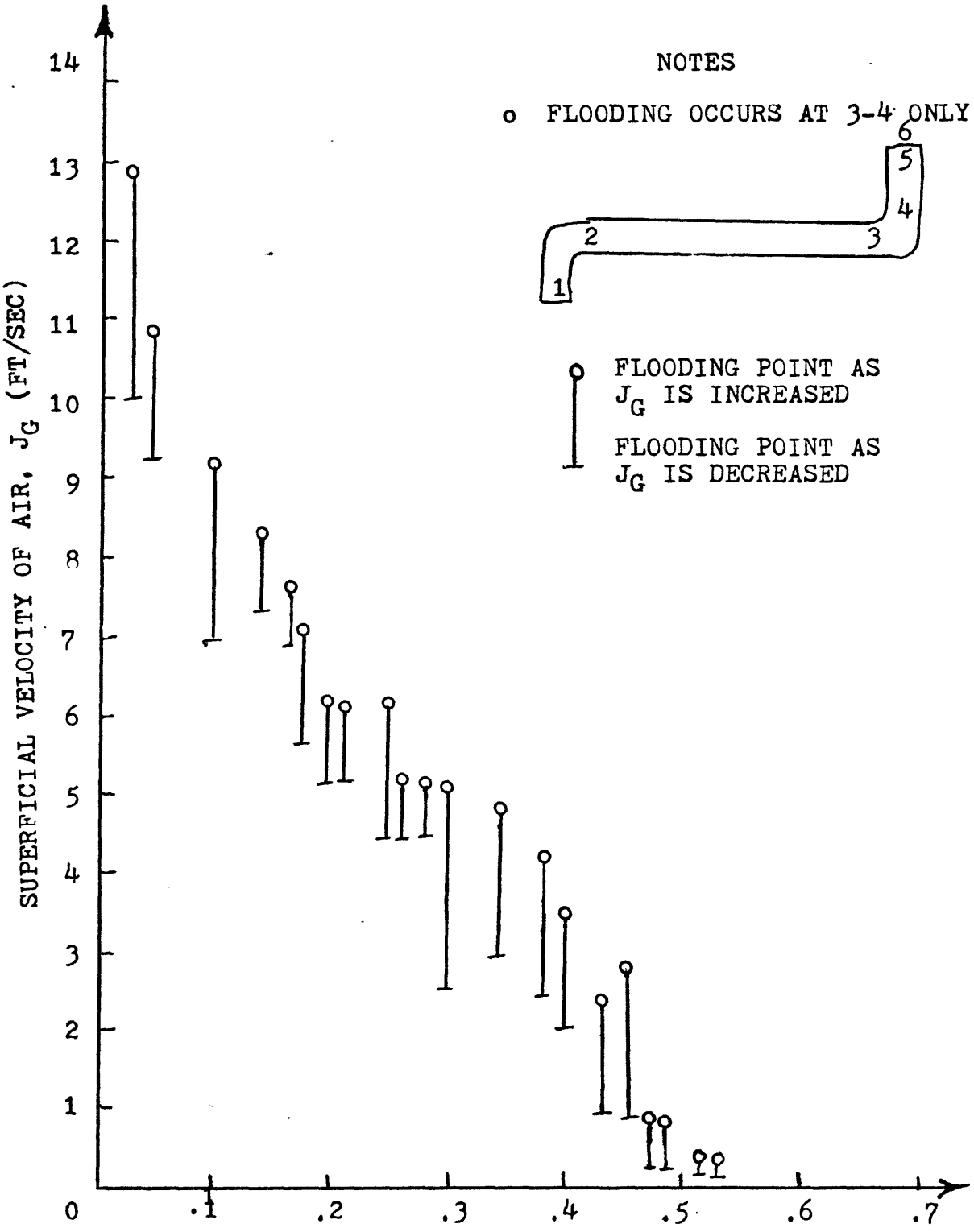

FIGURE 11. FLOODING CURVE FOR CONFIGURATION D

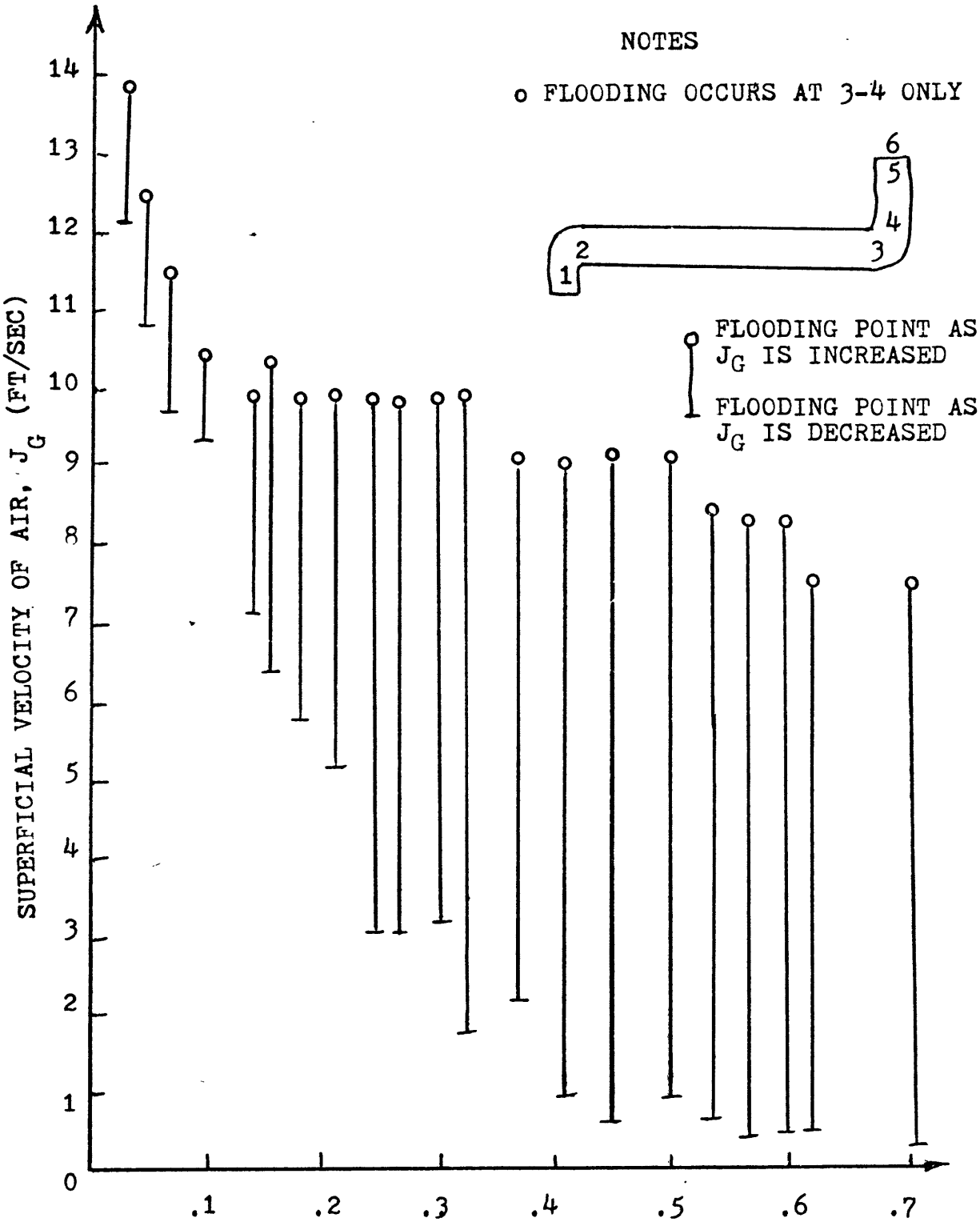

FIGURE 12. FLOODING CURVE FOR CONFIGURATION E

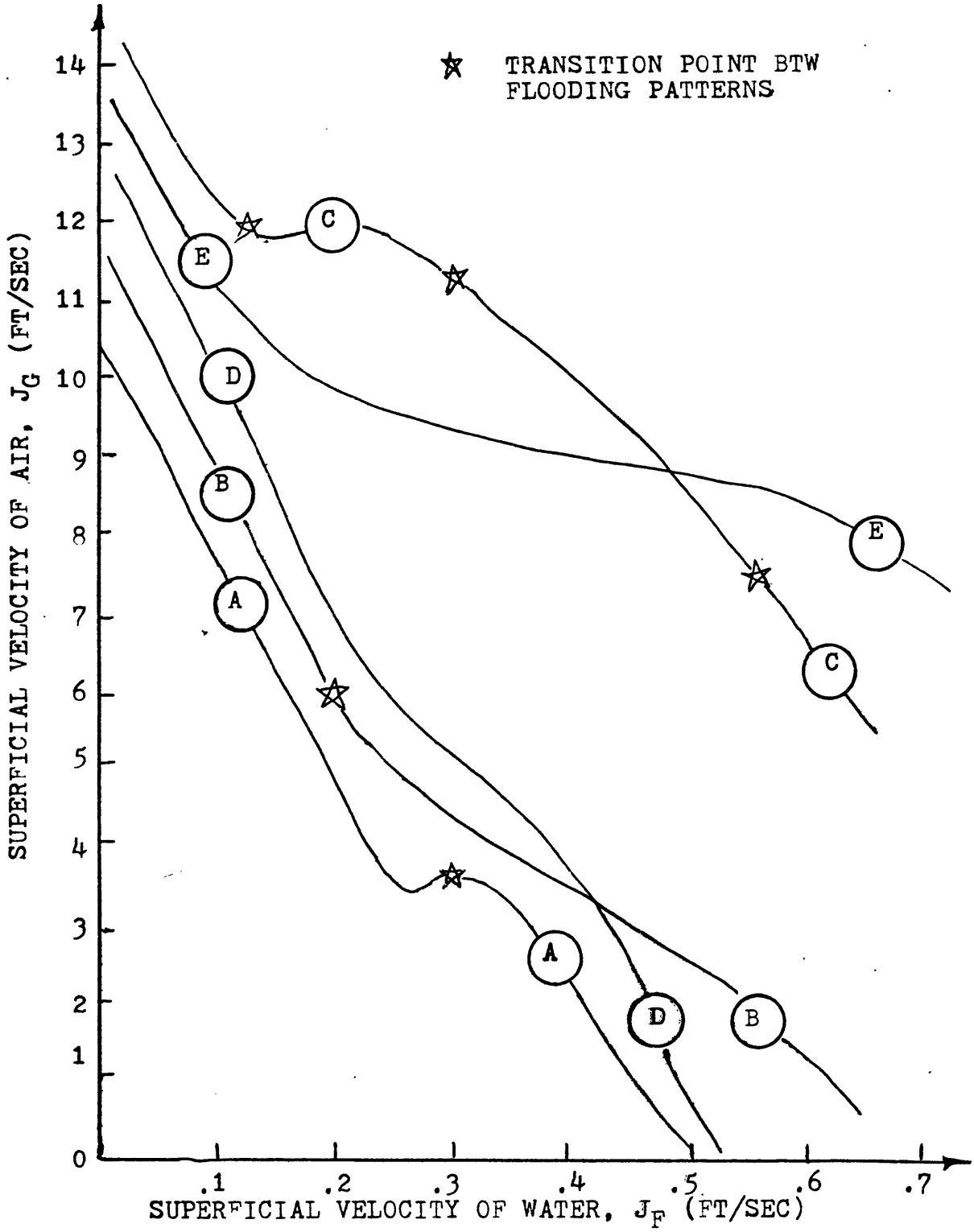

FIGURE 13. COMPOSITE PLOT OF FLOODING CURVES AS J_G IS INCREASED FOR CONFIGURATIONS A,B,C,D&E

back at both locations.

Configuration E is the closest geometric simulation of an actual reactor hot leg. Flooding data for configuration E was plotted on the basis of the square roots of the non-dimensional superficial velocities in Figure 14 in order to compare the results to Wallis's correlation. For J_F^* equal to zero, J_G^* or C is approximately equal to five. The slope of the non-dimensional flooding curve is approximately 1.7. This is reasonably close to Wallis's predictions. Wallis found C to be between .75 and 1 and m to be unity for vertical pipes. The range of hystersis for Configuration E was excessively high.

Further tests were performed on Configuration E to determine the liquid Froude numbers for the upper and lower air flow flooding limits for five different water flow rates. Wallis based his correlations on J_G^* and J_F^* which are analogous to the Froude number. For Fr greater than unity, the flow is supercritical and the force of water flow is greater than the gravity forces. For Fr less than unity, the flow is subcritical. Figure 15 illustrates the method used to calculate the Froude numbers. Table 1 compares the difference in flooding limits with the difference in liquid Froude numbers for several water flow rates. For the flow rates with the highest hystersis effects, the water flow was subcritical at the higher limit and supercritical at the lower limit. The change from subcritical to supercritical flow may account for the wide range of hystersis.

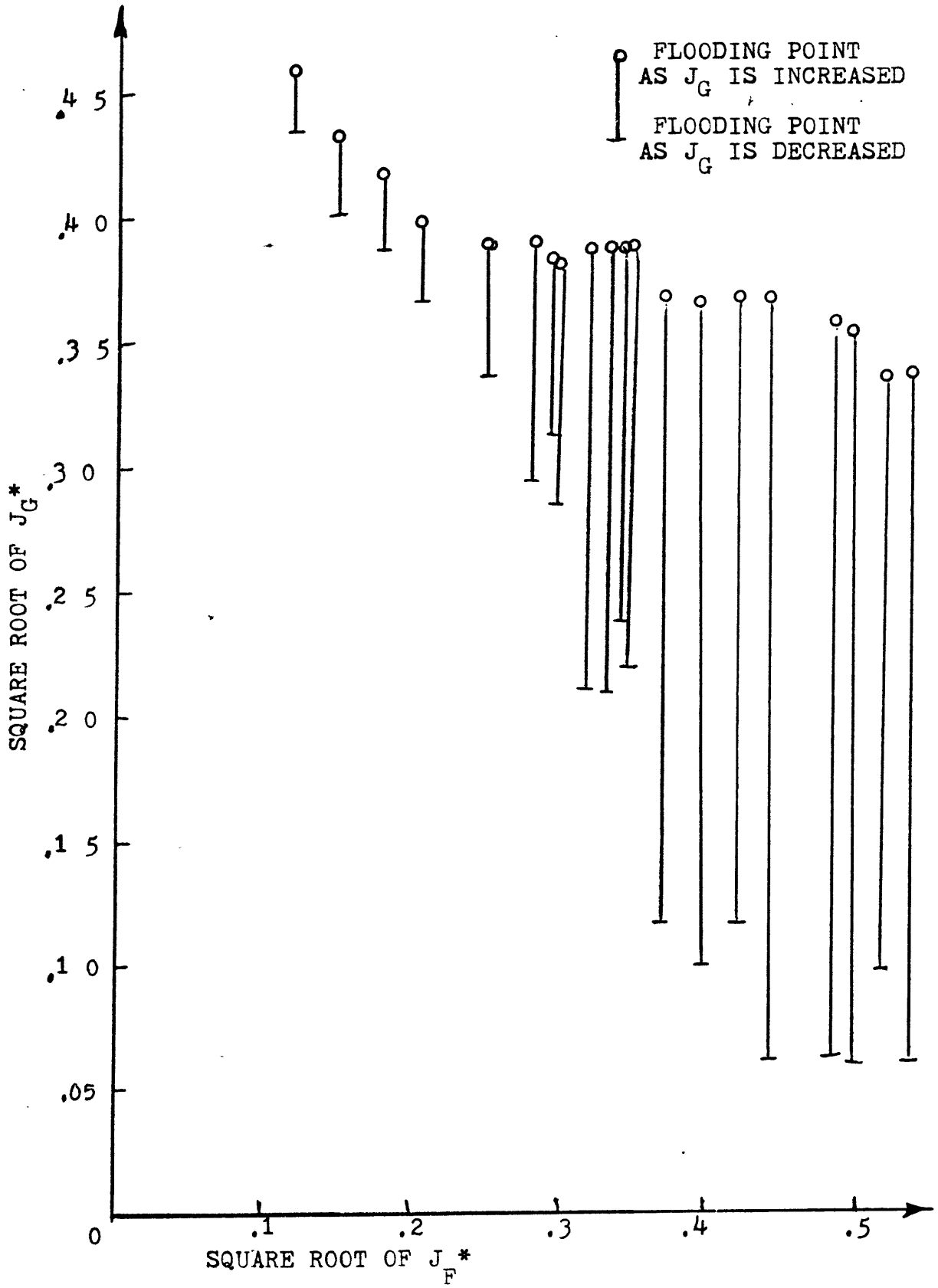

FIGURE 14. FLOODING CURVE BASED ON DIMENSIONLESS SUPERFICIAL VELOCITIES FOR CONFIGURATION E.

TABLE 1. EFFECT OF LIQUID FROUDE NUMBER ON RANGE OF HYSTERSIS FOR CONFIGURATION E

J_F ft/sec	VALUES FOR FLOODING POINT AS J_G IS INCREASED			VALUES FOR FLOODING POINT AS J_G IS DECREASED			DIFFERENCE IN J_G LIMITS
	h_{max}-ft	J_G-ft/sec	Fr	h_{max} ft	J_G-ft/sec	Fr	
.10	10.5	.063	.21	9.3	.083	.12	11%
.21	10.5	.083	.26	6.3	.15	.15	40%
.28	10.1	.083	.34	5.2	.10	.28	48%
.39	9.3	.063	.80	3.0	.15	.26	68%
.48	9.3	.052	1.37	2.1	.13	.28	77%
.60	9.3	.052	1.79	1.0	.13	.36	89%
.64	8.7	.063	1.33	.6	.15	.32	93%

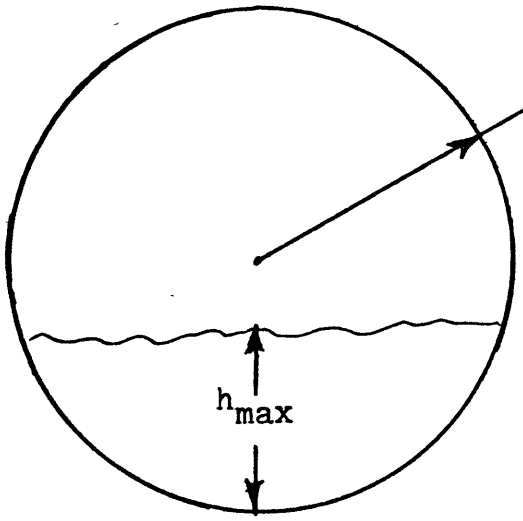

$$Fr = \frac{J_F \, A_{TOTAL}}{A_{WATER}\sqrt{g h_{max}}}$$

$$= .0038 \, \frac{J_F}{A_{WATER}\sqrt{h_{max}}}$$

FIGURE 15. SCHEMATIC TO ILLUSTRATE CALCULATION OF FROUDE NUMBERS

CONCLUSION

The results show that the geometry of the hot leg has a significant effect on the flooding limit. The flooding limits as J_G was increased for all the configurations were reasonably close to Wallis's results for vertical tubes. The range of hystersis, however, was unusually high for two of the configurations. It is possible that this is the result of a change in water flow from supercritical to subcritical as J_G is decreased.

Theses results suggest that further studies with geometrically identical models are needed to determine the flooding curve for a particular hot leg geometry.

Acknowledgements

I would like to thank Professor Griffith for his help and encouragement. Special thanks to Fred Johnson for building and maintaining the test apparatus.

REFERENCES

Fox and MacDonald, Introduction to Fluid Mechanics, John Wiley, New York, 1978.

Gouse, S. William Jr., "An Introduction to Two-Phase Gas Liquid Flow", Notes for Special Summer Program in Two Phase Flow, MIT, 1964.

Wallis, Graham, One Dimensional Two-Phase Flow, McGraw Hill, New York, 1969.

Wallis, Graham, "Flooding Phenomena in Two-Phase Flow", Notes for Special Summer Program in Two-Phase Gas-Liquid Flow, MIT, 1964.